



Can amide proton transfer-weighted imaging differentiate tumor grade and predict Ki-67 proliferation status of meningioma?

Hao Yu^{1,2} · Xinrui Wen³ · Pingping Wu⁴ · Yueqin Chen¹ · Tianyu Zou⁵ · Xianlong Wang² · Shanshan Jiang^{2,6} · Jinyuan Zhou⁶ · Zhibo Wen²

Received: 24 October 2018 / Revised: 15 January 2019 / Accepted: 15 February 2019 / Published online: 18 March 2019
© European Society of Radiology 2019

Abstract

Objectives To determine the utility of the amide proton transfer-weighted MR imaging in differentiating the WHO grade and predict proliferative activity of meningioma.

Methods Fifty-three patients with WHO grade I meningiomas and 26 patients with WHO grade II meningiomas underwent conventional and APT-weighted sequences on a 3.0 Tesla MR before clinical intervention. The APT-weighted (APT_w) parameters in the solid tumor region were obtained and compared between two grades using the *t* test; the receiver operating characteristic (ROC) curve was used to assess the best parameter for predicting the grade of meningiomas. Pearson's correlation coefficient was calculated between the APT_w_{max} and Ki-67 labeling index in meningiomas.

Results The APT_w_{max} and APT_w_{mean} values were not significantly different between WHO grade I and grade II meningiomas ($p = 0.103$ and $p = 0.318$). The APT_w_{min} value was higher and the APT_w_{max-min} value was lower in WHO grade II meningiomas than in WHO grade I tumors ($p = 0.027$ and $p = 0.019$). But the APT_w_{min} was higher and the APT_w_{max-min} was lower in microcystic meningiomas than in WHO grade II meningiomas ($p = 0.001$ and $p = 0.006$). The APT_w_{min} combined with APT_w_{max-min} showed the best diagnostic performance in predicting the grade of meningiomas with an AUC of 0.772. The APT_w_{max} value was positively correlated with Ki-67 labeling index ($r = 0.817$, $p < 0.001$) in meningiomas; the regression equation for the Ki-67 labeling index (%) (Y) and APT_w_{max} (%) (X) was $Y = 4.9 \times X - 12.4$ ($R^2 = 0.667$, $p < 0.001$).

Conclusion As a noninvasive imaging method, the ability of APT_w-MR imaging in differentiating the grade of meningiomas is limited, but the technology can be used to predict the proliferative activity of meningioma.

Key Points

- The APT_w_{min} value was higher and the APT_w_{max-min} value was lower in WHO grade II meningioma than in grade I tumors.
- The APT_w_{min} value was higher and the APT_w_{max-min} value was lower in microcystic meningiomas than in WHO grade II meningiomas.
- The APT_w_{max} value was positively correlated with meningioma proliferation index.

Keywords Magnetic resonance imaging · Amide proton transfer · Meningioma · Tumor grading · Cell proliferation

Hao Yu and Xinrui Wen contributed equally to this work.

✉ Zhibo Wen
zhibowen@163.com

¹ Department of Radiology, Affiliated Hospital of Jining Medical University, Jining Medical University, Guhuai Road No. 89, Rencheng District, Jining 272029, Shandong, China

² Department of Radiology, Zhujiang Hospital, Southern Medical University, Gongye Road M No. 253, Haizhu District, Guangzhou 510282, Guangdong, China

³ Department of Neurology, Zhujiang Hospital, Southern Medical University, Gongye Road M No. 253, Haizhu District, Guangzhou 510282, Guangdong, China

⁴ Department of Clinical Laboratory, Jining NO. 1 People's Hospital, 6 Jiankang Road, Jining 272011, China

⁵ Department of Radiology, Weihai Municipal Hospital, Heping Road M No.70, Weihai 264200, Shandong, China

⁶ Division of MR Research, Department of Radiology, Johns Hopkins University School of Medicine, 600N. Wolfe Street, Park 336, Baltimore, MD 21287, USA

Abbreviations

APT	amide proton transfer
APTw	APT-weighted
CEST	chemical exchange–based saturation transfer
CNAWM	contralateral normal-appearing white matter
Gd	gadolinium
H&E	hematoxylin and eosin
N/C	nucleus to cytoplasm ratio
ROI	region of interest

According to CBTRUS, there are 15 subtypes of meningiomas that constitute approximately 36.7% of all primary central nervous system neoplasms [1]. Most meningiomas are benign tumor classified as WHO grade I and the recurrence are infrequent, nearly 5% are WHO grade II/III tumors which behave more aggressively [2]. Surgical resection is the first choice for the treatment of meningioma, but surgery is invasive treatment; for most of benign meningiomas with diameter < 3 cm, close follow-up is a better management [3]. Ki-67 is a proliferation-related nuclear antigen that indicates the speed of tumor growth [4]. Previous studies have suggested that meningiomas with Ki-67 labeling index $\geq 3\%$ are prognostic for an increased risk of progression and recurrence [5]. Therefore, differentiating meningioma grade and predicting Ki-67 proliferation status preoperatively would be helpful for therapeutic planning.

Conventional and advanced MRI techniques can provide sufficient information to diagnose a meningioma. However, it has a limited diagnostic specificity in differentiating meningioma grade and predicting proliferation potential [6–11]. Amide proton transfer–weighted (APTw) MRI is a novel molecular MRI technique based on chemical exchange–based saturation transfer (CEST) and applied to imaging through the exchange between amide protons of mobile proteins and protons of bulk water [12]. The APTw signal is mainly related to cell density and endogenous mobile proteins [13, 14]. As an imaging biomarker, worthwhile results have been reported across various research, in grading glioma [15, 16], distinguishing treatment effects from tumor recurrence [17, 18], differentiating glial neoplasms from other intracranial tumor [13, 19], and distinguishing cancerous tissues in the prostate and breast [20, 21] and in other non-oncological diseases [22–24]. However, this technique is rarely used in meningioma, and only one investigator has reported using APTw-MR imaging to assess meningioma [25]. Therefore, the purpose of this study was to determine the utility of APT-weighted MRI in differentiating the tumor grade and proliferative activity of meningioma.

Materials and methods

Study population

The institutional review board of our hospital approved this retrospective study, and each patient signed the informed consent. Ninety-three patients suspected meningiomas were recruited and underwent conventional and APT-weighted MRI from May 2014 to June 2018. Eighty-six patients were pathologically diagnosed as meningiomas. Seven patients were excluded for poor-quality APTw images. Therefore, 79 patients were included in this study.

MR imaging

Imaging studies were performed on a 3.0 T MRI system (Achieva 3.0 T; Philips Medical Systems, Best, Netherlands) before clinical intervention. A body coil was used for radiofrequency (RF) transmission, and a 16-channel head coil was used for signal reception. Conventional MR images were acquired according to the routine brain tumor protocol in our hospital and included axial T₁-weighted imaging (repetition time (ms)/echo time (ms), 400/20), axial T₂-weighted imaging (repetition time (ms)/echo time (ms), 2800/105), and axial fluid-attenuated inversion recovery (FLAIR) imaging (repetition time (ms)/echo time (ms)/inversion recovery time (ms) 8000/204/2200). Then, axial, coronal, and sagittal gadolinium–enhanced T₁-weighted images were obtained after a contrast agent (Gd-DTPA; 0.2 ml/kg body weight; Magnevist; Bayer Schering, Guangzhou, China) was injected. Other imaging parameters were as follows: field of view, 240 × 240 mm²; slice thickness, 5 mm; gap, 2 mm; and matrix, 512 × 512. The 2D fat-suppressed, fast spin-echo APTw pulse sequence was performed at one T₂-weighted image slice showing the maximum area of the tumor before the Gd-T₁-weighted image. The APTw images were acquired with a multi-offset (offsets = 0, ± 0.25, ± 0.5, ± 0.75, ± 1, ± 1.5, ± 2, ± 2.5, ± 3, ± 3.25, ± 3.5, ± 3.75, ± 4, ± 4.5, ± 5, and ± 6 ppm), multi-acquisition protocol with a pulse-train radiofrequency saturation (duration time = 800 ms; interpulse delay = 10 ms; power level = 2 μT). The protocol was repeated 8 times at an offset of ± 3.5 ppm to increase the signal-to-noise ratio of the APTw images. In addition, an image that did not exert a saturated pulse was acquired for signal normalization, and an image that exerted a saturated pulse at the offset of 15.6 ppm was acquired to calculate the conventional magnetization transfer ratio (MTR) value. The detailed imaging parameters were as follows: sensitivity-encoding factor = 2, repetition time = 3 s; echo time = 11 ms; field of view, 240 × 240 mm²; section thickness = 6 mm; matrix = 128 × 64; and voxel size = 1.65 × 3.15 × 6.00 mm³. The total acquisition time was 192 s.

Image analysis

The APTw raw data were analyzed using interactive data language written in the IDL program (Research Systems, Inc., Boulder, CO, USA). First, the normalized saturated signal intensity curve (S_{sat}/S_0 , where S_{sat} and S_0 were the signal intensities obtained with and without selective saturation, respectively), known as the Z-spectrum, was calculated as a function of the saturation frequency offset. As described previously [26], the B_0 field inhomogeneity effect was corrected. To reduce the contributions from conventional magnetization, transfer contrast and direct saturation of bulk water, a B_0 -corrected Z-spectrum was used to analyze the magnetization transfer ratio asymmetry (MTR_{asym}) as follows: $\text{MTR}_{\text{asym}} = S_{\text{sat}}(-\text{offset})/S_0 - S_{\text{sat}}(+\text{offset})/S_0$. The APTw signal was calculated as MTR_{asym} (3.5 ppm).

Two experienced neuroradiologists (X.W. and S.J., who had 11 and 10 years of experience in neuroradiology, respectively) analyzed the conventional and APTw images. According to the previous study [27], the tumor signal intensity on T_1 - and T_2 -weighted images, tumor enhancement type on gadolinium-enhanced T_1 -weighted image, and tumor volume were recorded; we also calculated the edema index (EI) which is defined as $\text{EI} = V_{\text{tumor} + \text{edema}}/V_{\text{tumor}}$ [28]. Five regions of interest (ROIs) were distributed based on the Gd- T_1 WI and T_2 WI co-registered with the APTw image [29]; the size of each ROI was fixed at 15 pixels (Fig. 1). Necrosis, cystic cavities, large vessels, calcification, and hemorrhagic components were excluded. For each patient, the APTw values in five ROIs (APT_{w_1} , APT_{w_2} ... APT_{w_5}) were recorded. Then, the maximum APTw value of them ($\text{APT}_{w_{\text{max}}}$), the minimum APTw value of them ($\text{APT}_{w_{\text{min}}}$), the maximum APTw value–minimum APTw value ($\text{APT}_{w_{\text{max-min}}}$), and $(\text{APT}_{w_1} + \text{APT}_{w_2} + \dots + \text{APT}_{w_5})/5$ ($\text{APT}_{w_{\text{mean}}}$) were determined.

Pathological data acquisition

The neurosurgeon (S.Z. who had 25 years of experience in neurosurgery) obtained specimens from the tumor region that showed the highest signal on APTw imaging during surgery. One neuropathologist (Y.L. who had 6 years of experience in neuropathology) reviewed specimens after hematoxylin and eosin (H&E) and Ki-67 antigen staining and pathological diagnosis was made based on the 2016 World Health Organization (WHO) classification of tumors of the central nervous system (CNS). For diagnosis WHO grade II meningioma, the following criteria are used: 4 to 19 mitoses per 10 high-power fields (HPF), the presence of brain invasion, or the presence of at least 3 of other 5 features: sheet-like growth, loss of whirling or fascicular architecture, hypercellularity, prominent nucleoli, spontaneous necrosis, and tumor clusters with high nuclear to cytoplasmic ratio (N/C) [30]. Additionally, the Ki-67 labeling index was estimated.

Statistical analysis

Statistical analyses were performed using a statistical analysis software (SPSS19.0). The patient's gender, tumor signal intensity, and enhancement type on conventional MRI between WHO grade I and grade II were analyzed using the chi-square test. The comparisons between patient's age, tumor volume, EI, $\text{APT}_{w_{\text{max}}}$, $\text{APT}_{w_{\text{min}}}$, $\text{APT}_{w_{\text{max}}}-\text{APT}_{w_{\text{min}}}$, $\text{APT}_{w_{\text{mean}}}$ values, and the Ki-67 labeling index for grade I and grade II tumors were performed using an independent samples t test, followed by the Levene test. Receiver operating characteristic (ROC) curves were generated for each APTw parameter value to assess the areas under the curve (AUCs) and determine the optimal cutoff values for discrimination between two clinical entities. AUC values of < 0.7 , $0.7-0.9$, and > 0.9 indicated low, medium, and high diagnostic performance, respectively. Logistic regression was applied to evaluate the diagnostic

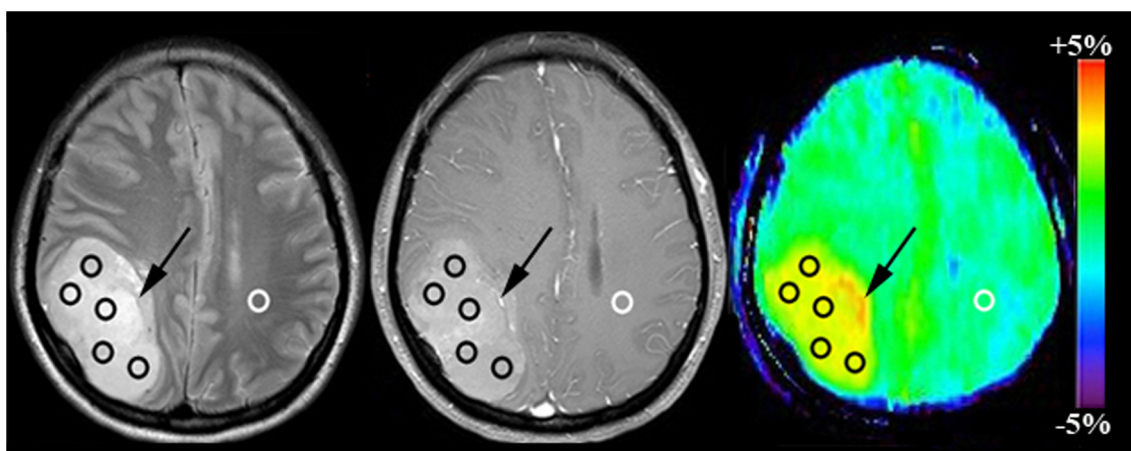


Fig. 1 Example of the placement of ROIs. Five ROIs were placed in the Gd-enhancing tumor part (black circle) and one ROI was placed in the CNAWM (white circle) based on the co-registered traditional images. The vessel-related image artifact can be seen (black arrow)

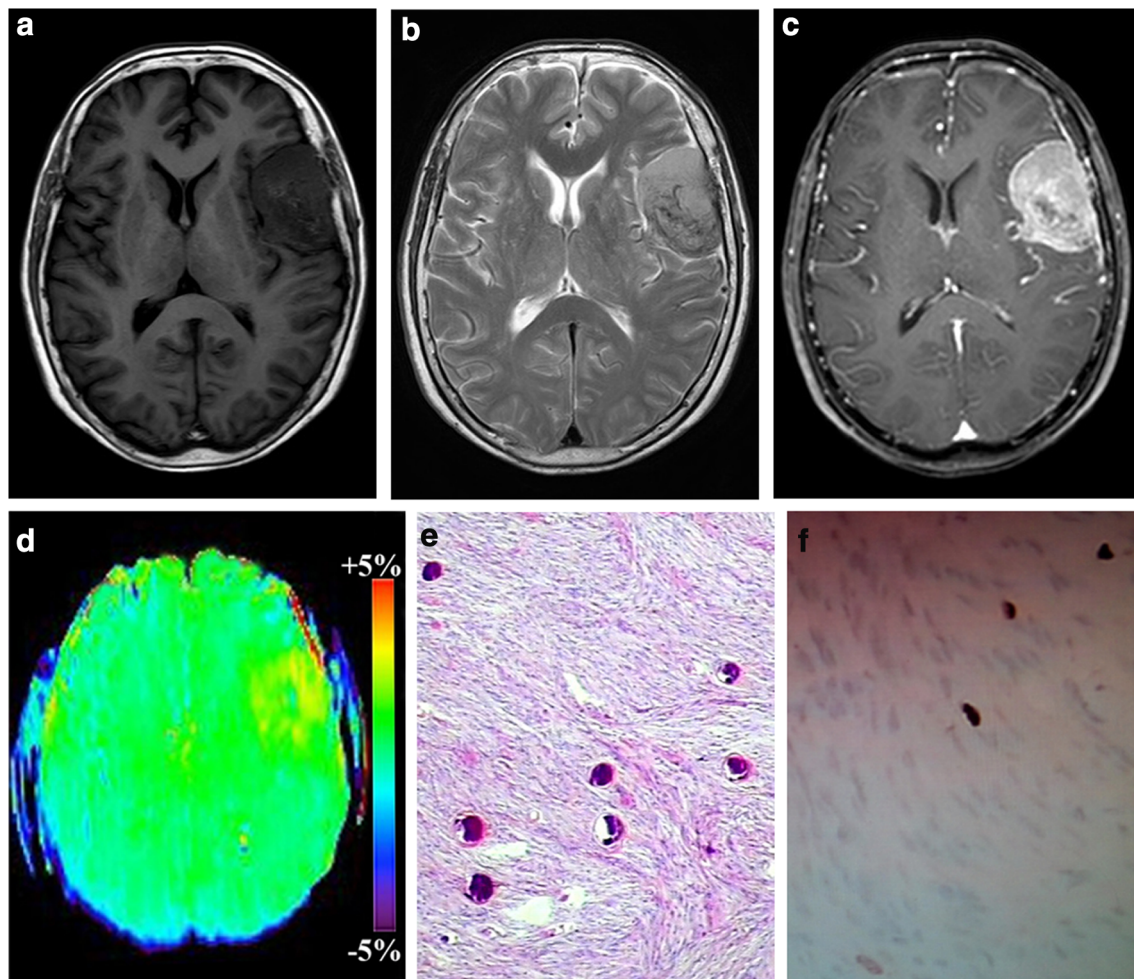


Fig. 2 A 39-year-old male with fibroblastic meningioma (WHO grade I). (**a–c**) The mass was located in the left frontal, exhibiting isointense on T₁WI, hyperintense on T₂WI, and heterogeneous enhancement. **d** In the APTw image, the mass exhibiting heterogeneous signal and the tumor identified approximately equal as in the Gd-T₁weighted images. The

APT_w_{max} = 3.18%, APT_w_{min} = 2.06% APT_w_{max-min} = 1.12%, APT_w_{mean} = 2.63%. The part rich in psammoma body showed hypointense on T₁WI and T₂WI, and isointense on APTw image (black arrow). (**e**) HE staining showed many psammoma body in the tumor. **f** Ki-67 labeling index was 3%

performance of the combination indices. Pearson's correlation coefficient was used to analyze the association between APT_w_{max} and Ki-67 labeling index of all meningioma. Linear regression equation was established to evaluate the Ki-67 labeling index. $P < 0.05$ was considered to be a statistically significant difference for all tests.

Results

Fifty-three patients were pathologically diagnosed with WHO grade I meningioma (21 males, 32 females; age range, 19–73 years; mean age, 48.9 ± 12.3 years), including 19 fibroblastic, 20 meningothelial, 9 transitional, and 5 microcystic meningiomas. Twenty-three out of 53 cases found psammoma bodies. Twenty-six patients were pathologically diagnosed with WHO grade II meningioma (11 males, 15 females; age range, 18–67 years; mean age, 53.2 ± 11.3 years), including

23 atypical, 2 clear-cell, and 1 chordoid meningiomas. Five out of 26 cases found psammoma bodies.

The gender ratio and age was not significantly different between WHO grade I and WHO grade II meningiomas ($p = 0.947$ and $p = 0.095$, respectively). The proliferation index in grade II meningiomas was significantly higher than that in grade I tumors ($5.85\% \pm 3.18\%$ vs. $4.06\% \pm 2.31\%$, $p = 0.015$).

For 53 cases WHO grade I meningiomas, 17/53 cases showed hypointense and 36/53 cases showed isointense on T₁-weighted image, 3/53 cases showed hypointense, 21/53 cases showed isointense, and 29/53 cases showed hyperintense on T₂-weighted image. On the Gd-T₁W image, 42/53 cases showed homogenous enhancement and 11/53 showed heterogeneous enhancement. The tumor volume ranged from 28.3 to 40.8 mm³. When the quantitative EI was measured, 21 cases were $EI \leq 1.5$, 28 cases $1.5 < EI \leq 3$, and 4 cases $EI > 3$. For 26 cases of WHO grade II meningiomas, 12/26 cases showed hypointense and 14/26 cases showed isointense on

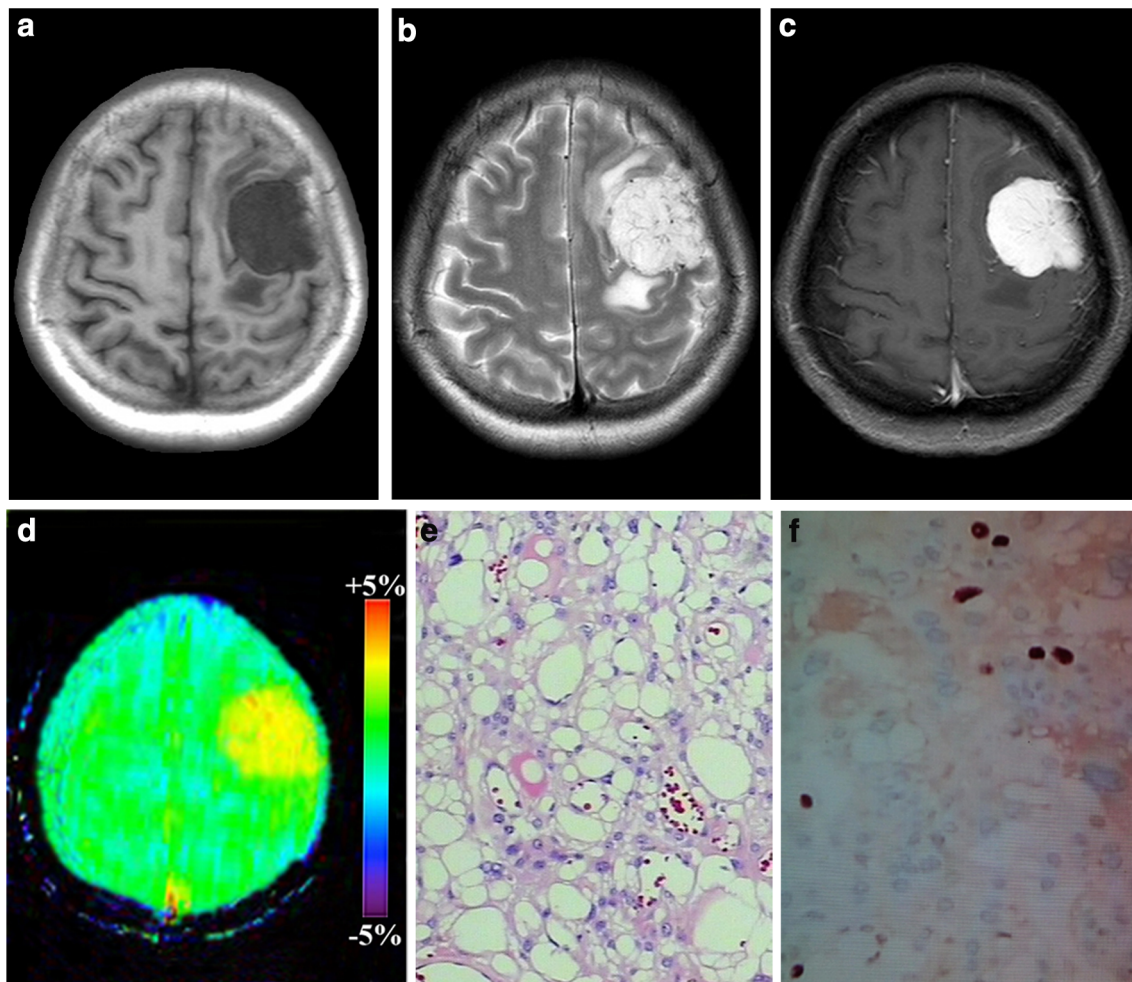


Fig. 3 A 54-year-old female with microcystic meningioma (WHO grade I). (a–c) The mass was located in the left frontal, exhibiting hypointense on T₁WI, hyperintense on T₂WI, and obvious homogeneous enhancement. (d) In the APTw image, the mass exhibiting homogeneous signal

and the tumor identified approximately equal as in the Gd-T1-weighted images. $APT_{w_{max}} = 3.58\%$, $APT_{w_{min}} = 3.22\%$, $APT_{w_{max-min}} = 0.36\%$, $APT_{w_{mean}} = 3.45\%$. (e) HE staining showed numerous microcystic spaces in the tumor. (f) Ki-67 labeling index was 5%

T₁-weighted image. One out of 26 cases showed hypointense, 8/26 cases showed isointense, and 17/26 cases showed hyperintense on T₂-weighted image. On the Gd-T₁-weighted image, 12/26 cases showed homogenous enhancement and 14/26 showed heterogeneous enhancement. The tumor volume ranged from 31.8 to 41.2 mm³. When the quantitative EI was measured, 6 cases were $EI \leq 1.5$, 18 cases $1.5 < EI \leq 3$, and 2 cases $EI > 3$. There was no significant difference in tumoral signal on T₁- and T₂-weighted image ($p = 0.320$, $p = 0.661$ respectively), tumoral volume ($35.2 \text{ mm}^3 \pm 5.2 \text{ mm}^3$ vs. $36.7 \text{ mm}^3 \pm 4.5 \text{ mm}^3$, $p = 0.149$), and EI value (1.70 ± 0.86 vs. 2.01 ± 0.71 , $p = 0.119$) between WHO grade I and WHO grade II tumors. However, WHO grade II meningiomas showed heterogeneous enhancement than grade I meningiomas ($p = 0.004$).

Both WHO grade I and WHO grade II meningiomas identified by APTw imaging were approximately equal to those identified on the Gd-T₁-weighted images. Compared with the CNAWM, for 12/53 WHO grade I meningioma cases, the Gd-

enhancing tumor parenchyma showed heterogeneous signal on APTw images (Fig. 2). For 41/53 WHO grade I meningioma cases, the Gd-enhancing tumor parenchyma overall showed hyperintense on APTw images; within them, 5/41 meningiomas showed more homogeneous hyperintense than their partners. Interestingly, 5 meningiomas were confirmed as microcystic meningiomas by pathology (Fig. 3). Compared with the CNAWM, for 26/26 WHO grade II meningioma cases, the Gd-enhancing tumor parenchyma overall showed homogeneous hyperintense on APTw images (Fig. 4).

The values of the APTw parameters for the two groups are summarized in Table 1. No significant differences in $APT_{w_{max}}$ value ($p = 0.103$) and $APT_{w_{mean}}$ value ($p = 0.318$) were identified between the WHO grade I and WHO grade II tumors. The $APT_{w_{min}}$ values were higher in WHO grade II meningiomas than in WHO grade I tumors ($p = 0.027$). The $APT_{w_{max-min}}$ values were lower in WHO grade II meningiomas than in WHO grade I meningiomas ($p = 0.019$). However, the $APT_{w_{min}}$ was higher and the $APT_{w_{max-min}}$ was lower in 5

cases of microcystic meningiomas than in WHO grade II meningiomas ($p = 0.001$ and $p = 0.006$).

The diagnostic performance of APTw parameters in prediction of the grade of meningiomas is summarized in Table 2. It was showed that APTw_{min} combined with APTw_{max-min} had the highest AUC of 0.772 (Fig. 5); when the APTw_{min} higher than 2.58% was combined with APTw_{max-min} lower than 0.89%, the lesion was diagnosed as a WHO grade II, the sensitivity was 67.9%, and the specificity was 96.2%.

The APTw_{max} value was positively correlated with Ki-67 labeling index in meningiomas ($r = 0.817$, $p < 0.001$). The regression equation for the Ki-67 labeling index (%) (Y) and APTw_{max} (%) (X) among meningiomas was $Y = 4.9 \times X - 12.4$ ($R^2 = 0.667$, $p < 0.001$). According to the

Table 1 Comparing difference of APTw within WHO grade I and WHO grade II meningiomas

	WHO grade I	WHO grade II	p
APT _w _{max} (%)	3.39 ± 0.45	3.57 ± 0.44	0.103
APT _w _{min} (%)	2.50 ± 0.49	2.77 ± 0.47	0.027
APT _w _{mean} (%)	3.06 ± 0.45	3.17 ± 0.47	0.318
APT _w _{max-min} (%)	0.89 ± 0.19	0.78 ± 0.16	0.019

Abbreviations: APT_w_{max}, amide proton transfer-weighted max; APT_w_{min}, amide proton transfer-weighted min; APT_w_{mean}, amide proton transfer-weighted mean; APT_w_{max-min}, amide proton transfer-weighted max–amide proton transfer-weighted min

regression equation, the APTw_{max} value was 3.14% when the Ki-67 labeling index was 3%.

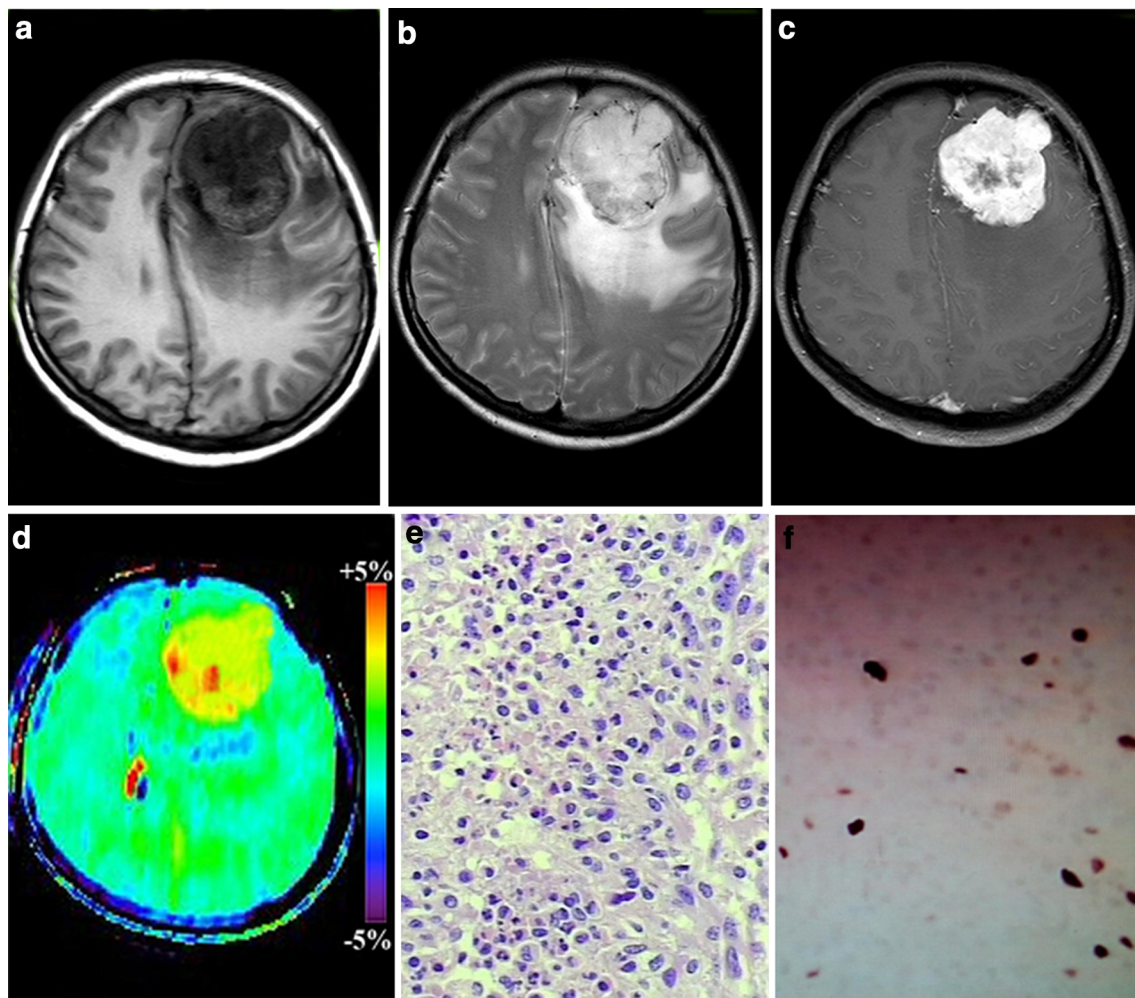


Fig. 4 A 49-year-old female with atypical meningioma (WHO grade II). (a–c) The mass was located in the left frontal, exhibiting hypointense on T₁WI, hyperintense on T₂WI, and obvious heterogeneous enhancement. (d) In the APTw image, the mass exhibiting relative homogeneous signal and the tumor identified approximately equal as on the Gd-T1-weighted

images the APTw_{max} = 4.02%, APTw_{min} = 3.11% APTw_{max-min} = 0.71%, APTw_{mean} = 3.87%. Necrosis-related image artifact (black arrow) and ventricle-related image artifact (white arrow) can be seen. (e) HE staining showed high nuclear to cytoplasmic ratio cells are arranged loss of whirling or fascicular architecture. (f) Ki-67 labeling index was 10%

Table 2 Diagnostic performance of APTw parameters in prediction the grade of meningioma

	Cutoff value	Sensitivity (%)	Specificity (%)	AUC
APT _w _{min}	2.58	64.2	69.2	0.673
APT _w _{max-min}	0.89	56.6	92.3	0.708
APT _w _{min} + APT _w _{max-min}	— ^a	67.9	96.2	0.772

Abbreviations: APT_w_{min}, amide proton transfer–weighted min; APT_w_{max-min}, amide proton transfer–weighted max–amide proton transfer–weighted min; AUC, area under the curve

^a The combined cutoff values were the same as the individual index above

Discussion

Consistent with Lin's report [27], both groups had a female predominance and heterogeneous enhancement was more common in WHO grade II meningiomas in this study. Lin reported that high-grade meningiomas were more common in older people that is not supported by this study; maybe it was a result of the bias of the sample. Consistent with Soon's report [31], the tumor volume of WHO grade II meningiomas was not significantly higher than that of grade I meningiomas. Additionally, Soon found grade II meningiomas have significantly higher volumetric growth rate than grade I meningioma; the statement was not discussed in this study. EI was not different between WHO grade I and grade II meningiomas, because peritumoral edema in meningiomas was dependent on AQP-4 expression and the expression of AQP-4 was not related with tumor grade [32].

Compared with CNAWM, both WHO grade I and grade II meningiomas showed completely hyperintense or

hyperintense mixed with isointense on APTw images. The lesions identified by APTw were approximately equal to those identified by Gd-T₁W images. Technically, the predominant factors that affected the APTw signal were cell density and mobile amide proton [26]; the tumor core had greater cell densities and mobile protein and peptide content than in CNAWM. This finding was particularly valuable for the meningioma patients without proper surgical indications, because potential central nervous system damage and nephrogenic systemic fibrosis caused by Gd deposition may be missed upon re-examination [33, 34].

For the meningiomas which demonstrated isointense on APTw images, we found they were richer in psammoma bodies, and the isointense region was larger, the psammoma bodies' content was richer, and maybe the psammoma bodies generate weaker APT effect. It was useful for predicting the hardness of the meningioma, because the psammoma bodies' content was richer and the masses were harder; then, the tumor would be more difficult to remove; it was helpful in making surgical plans.

The APT_w_{max} and APT_w_{mean} values of WHO grade II meningiomas were not statistically higher than grade I meningiomas. Pathologically, compared with WHO grade I meningiomas, the grade II meningiomas were associated with a higher cell density and N/C ratio [30]. According to previous studies, technically, higher cell density made WHO grade II generate stronger APT effect than WHO grade I meningioma. However, higher N/C ratio made WHO grade II generate weaker APT effect than WHO grade I meningioma [13, 26]. Perhaps this leads to an overlap between the APTw signal of meningiomas in different grades. The APT_w_{min} value was lower in grade I meningiomas. Pathologically, compared to WHO grade II meningiomas, the psammoma bodies which supposed to generate poor APT effect were more common in grade I meningiomas. As a parameter that indicated the APTw signal heterogeneity, the APT_w_{max-min} was lower in the WHO grade II meningioma than that in the WHO grade I meningioma. Pathologically, In WHO grade I meningioma, the shapes of the neoplastic cells were oval or spindle-shaped and formed whorls, fascicles, cords, or nodules. By contrast, specific patterns were rarely found in WHO grade II meningiomas [30]. Perhaps the special pathological structure resulted in more uneven distribution of mobile protein and peptide content in low-grade meningiomas than in their high-grade partners.

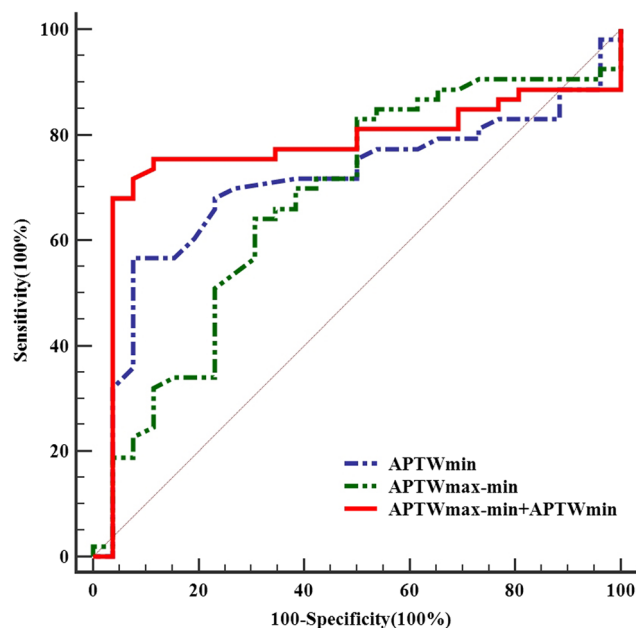


Fig. 5 Diagnostic performance of amide proton transfer (APT) parameters in differentiating the grade of meningioma. APT_w_{min} combined with APT_w_{max-min} showed the best diagnostic performance, with an AUC of 0.772, followed by APT_w_{max-min} of 0.708 and APT_w_{min} of 0.673

According to ROC analysis, even $APT_{w_{min}}$ combined with $APT_{w_{max-min}}$ has the best diagnostic performance in prediction of the grade of meningioma, but the sensitivity and specificity were only 67.9% and 96.2%; the performance of APT_{w-MRI} used for grading meningiomas was not as good as that in glioma [15]. Maybe the meningioma components were more complex than glioma components.

It is interesting that as WHO grade I meningiomas, the signal features of microcystic meningiomas were similar with those of WHO grade II meningiomas on the APT_{w-MR} images; quantifying the APT_{w} parameters, the $APT_{w_{min}}$ of microcystic meningioma was higher and the $APT_{w_{max-min}}$ was lower than that of grade II meningiomas. Histologically, numerous microcyst spaces were formed by tumor cells and extracellular substrates in microcystic meningiomas, and the spaces were filled with edematous fluid [35]. Maybe the mobile protein and peptide content in microcystic meningiomas are higher and the distribution is more homogeneous than those in high-grade meningioma. We hypothesize that besides the grade of the meningiomas, the subtype of the meningioma affects the APT_{w} signal either, and additional study is needed.

Compared with studies in gliomas using APT_{w-MRI} [36, 37], we found that $APT_{w_{max}}$ was positively correlated with Ki-67 labeling index in meningiomas either. According to the one-dimensional linear regression equation, when the $APT_{w_{max}}$ value is higher than 3.14%, Ki-67 labeling index is 3%, and thus, more enterprising presurgical planning should be considered.

This study had some limitations. First, there were only 7 subtypes of meningiomas and no WHO grade III meningiomas were recruited. Further exploration is needed to clarify the link between APT_{w} parameters and grade or subtypes as more cases and subtypes of meningiomas are recruited. Second, the APT_{w} sequence covered only one slice; as the 3D APT_{w-MRI} developed, additional cases will recruit using the 3D APT_{w} sequence to assess tumors comprehensively. Third, the neurosurgeon obtained the samples from target part according to his experience, so there was potential bias in acquisition the specimens; in the future, we will request the neurosurgeon take measure to obtain more accurate samples.

In conclusion, the APT_{w-MR} imaging used to differentiate the grades of meningiomas is limited; besides the grade of the meningioma, the subtypes also influence the APT signal, and $APT_{w_{max}}$ positively correlated with the Ki-67 proliferation status. Even the diagnostic performance was not good enough. As a supplementary MR technology, APT -weighted MRI would be providing a more comprehensive preoperative assessment of meningioma patients to benefit therapeutic decision-making in the clinic.

Funding This study is partially supported by grants from Natural Science Foundation of Guangdong Province (2014A030313271),

Guangdong Provincial Science and Technology Project (2014A020212726), Southern Medical University clinical research project (LC2016ZD028), and the National Institutes of Health (R01EB009731, R01CA166171).

Compliance with ethical standards

Guarantor The scientific guarantor of this publication is Zhibo Wen Ph.D., M.D.

Conflict of interest The authors of this manuscript declare no relationships with any companies, whose products or services may be related to the subject matter of the article.

Statistics and biometry No complex statistical methods were necessary for this paper.

Informed consent Written informed consent was obtained from all subjects (patients) in this study.

Ethical approval Institutional Review Board approval was obtained.

Methodology

- retrospective
- diagnostic or prognostic study
- performed at one institution

References

1. Ostrom QT, Gittleman H, Liao P et al (2017) CBTRUS statistical report: primary brain and other central nervous system tumors diagnosed in the United States in 2010-2014. *Neuro Oncol* 19:v1–v88
2. Kshetry VR, Ostrom QT, Kruchko C, Al-Mefty O, Barnett GH, Barnholtz-Sloan JS (2015) Descriptive epidemiology of World Health Organization grades II and III intracranial meningiomas in the United States. *Neuro Oncol* 17:1166–1173
3. Lin Z, Zhao M, Ren X et al (2017) Clinical features, radiologic findings, and surgical outcomes of 65 intracranial psammomatous meningiomas. *World Neurosurg* 100:395–406
4. Swiderska-Chadaj Z, Markiewicz T, Grala B, Lorent M (2016) Content-based analysis of Ki-67 stained meningioma specimens for automatic hot-spot selection. *Diagn Pathol* 11:93
5. Marciscano AE, Stemmer-Rachamimov AO, Niemierko A et al (2016) Benign meningiomas (WHO grade I) with atypical histological features: correlation of histopathological features with clinical outcomes. *J Neurosurg* 124:106–114
6. Lu Y, Xiong J, Yin B, Wen J, Liu L, Geng D (2018) The role of three-dimensional pseudo-continuous arterial spin labelling in grading and differentiating histological subgroups of meningiomas. *Clin Radiol* 73:176–184
7. Xing F, Tu N, Koh TS, Wu G (2017) MR diffusion kurtosis imaging predicts malignant potential and the histological type of meningioma. *Eur J Radiol* 95:286–292
8. Zikou A, Alexiou GA, Goussia A et al (2016) The role of diffusion tensor imaging and dynamic susceptibility perfusion MRI in the evaluation of meningioma grade and subtype. *Clin Neurol Neurosurg* 146:109–115
9. Surov A, Ginat DT, Sanverdi E et al (2016) Use of diffusion weighted imaging in differentiating between malignant and benign meningiomas. A multicenter analysis. *World Neurosurg* 88:598–602

10. Surov A, Gottschling S, Mawrin C et al (2015) Diffusion-weighted imaging in meningioma: prediction of tumor grade and association with histopathological parameters. *Transl Oncol* 8:517–523
11. Santelli L, Ramondo G, Della Puppa A et al (2010) Diffusion-weighted imaging does not predict histological grading in meningiomas. *Acta Neurochir (Wien)* 152:1315–1319 discussion 1319
12. Zhou J, Payen JF, Wilson DA, Traystman RJ, van Zijl PC (2003) Using the amide proton signals of intracellular proteins and peptides to detect pH effects in MRI. *Nat Med* 9:1085–1090
13. Jiang S, Yu H, Wang X et al (2016) Molecular MRI differentiation between primary central nervous system lymphomas and high-grade gliomas using endogenous protein-based amide proton transfer MR imaging at 3 tesla. *Eur Radiol* 26:64–71
14. Togao O, Kessinger CW, Huang G et al (2013) Characterization of lung cancer by amide proton transfer (APT) imaging: an in-vivo study in an orthotopic mouse model. *PLoS One* 8:e77019
15. Zou T, Yu H, Jiang C et al (2018) Differentiating the histologic grades of gliomas preoperatively using amide proton transfer-weighted (APTW) and intravoxel incoherent motion MRI. *NMR Biomed* 31
16. Togao O, Yoshiura T, Keupp J et al (2014) Amide proton transfer imaging of adult diffuse gliomas: correlation with histopathological grades. *Neuro Oncol* 16:441–448
17. Ma B, Blakeley JO, Hong X et al (2016) Applying amide proton transfer-weighted MRI to distinguish pseudoprogression from true progression in malignant gliomas. *J Magn Reson Imaging* 44:456–462
18. Zhou J, Tryggstad E, Wen Z et al (2011) Differentiation between glioma and radiation necrosis using molecular magnetic resonance imaging of endogenous proteins and peptides. *Nat Med* 17:130–134
19. Yu H, Lou H, Zou T et al (2017) Applying protein-based amide proton transfer MR imaging to distinguish solitary brain metastases from glioblastoma. *Eur Radiol* 27:4516–4524
20. Dula AN, Arlinghaus LR, Dortch RD et al (2013) Amide proton transfer imaging of the breast at 3 T: establishing reproducibility and possible feasibility assessing chemotherapy response. *Magn Reson Med* 70:216–224
21. Jia G, Abaza R, Williams JD et al (2011) Amide proton transfer MR imaging of prostate cancer: a preliminary study. *J Magn Reson Imaging* 33:647–654
22. Zhang H, Kang H, Zhao X et al (2016) Amide proton transfer (APT) MR imaging and magnetization transfer (MT) MR imaging of pediatric brain development. *Eur Radiol* 26:3368–3376
23. Tietze A, Blicher J, Mikkelsen IK et al (2014) Assessment of ischemic penumbra in patients with hyperacute stroke using amide proton transfer (APT) chemical exchange saturation transfer (CEST) MRI. *NMR Biomed* 27:163–174
24. Li C, Peng S, Wang R et al (2014) Chemical exchange saturation transfer MR imaging of Parkinson's disease at 3 tesla. *Eur Radiol* 24:2631–2639
25. Joo B, Han K, Choi YS et al (2018) Amide proton transfer imaging for differentiation of benign and atypical meningiomas. *Eur Radiol* 28:331–339
26. Wen Z, Hu S, Huang F et al (2010) MR imaging of high-grade brain tumors using endogenous protein and peptide-based contrast. *Neuroimage* 51:616–622
27. Lin BJ, Chou KN, Kao HW et al (2014) Correlation between magnetic resonance imaging grading and pathological grading in meningioma. *J Neurosurg* 121:1201–1208
28. Osawa T, Tosaka M, Nagaishi M, Yoshimoto Y (2013) Factors affecting peritumoral brain edema in meningioma: special histological subtypes with prominently extensive edema. *J Neurooncol* 111:49–57
29. Zhang Y, Heo HY, Lee DH et al (2016) Selecting the reference image for registration of CEST series. *J Magn Reson Imaging* 43:756–761
30. Louis DN, Perry A, Reifenberger G et al (2016) The 2016 World Health Organization classification of tumors of the central nervous system: a summary. *Acta Neuropathol* 131:803–820
31. Soon WC, Fountain DM, Koczyk K et al (2017) Correlation of volumetric growth and histological grade in 50 meningiomas. *Acta Neurochir (Wien)* 159:2169–2177
32. Gawlitza M, Fiedler E, Schob S, Hoffmann KT, Surov A (2017) Peritumoral brain edema in meningiomas depends on aquaporin-4 expression and not on tumor grade, tumor volume, cell count, or Ki-67 labeling index. *Mol Imaging Biol* 19:298–304
33. Collidge TA, Thomson PC, Mark PB et al (2007) Gadolinium-enhanced MR imaging and nephrogenic systemic fibrosis: retrospective study of a renal replacement therapy cohort. *Radiology* 245:168–175
34. Ramalho J, Castillo M, AlObaidy M et al (2015) High signal intensity in globus pallidus and dentate nucleus on unenhanced T1-weighted MR images: evaluation of two linear gadolinium-based contrast agents. *Radiology* 276:836–844
35. Seok JY, Kim NR, Cho HY, Chung DH, Yee GT, Kim EY (2014) Crush cytology of microcystic meningioma with extensive sclerosis. *Korean J Pathol* 48:77–80
36. Bai Y, Lin Y, Zhang W et al (2017) Noninvasive amide proton transfer magnetic resonance imaging in evaluating the grading and cellularity of gliomas. *Oncotarget* 8:5834–5842
37. Su C, Liu C (2017) Amide proton transfer imaging allows detection of glioma grades and tumor proliferation: comparison with Ki-67 expression and proton MR spectroscopy imaging. *AJNR Am J Neuroradiol* 38:1702–1709

Publisher's note Springer Nature remains neutral with regard to jurisdictional claims in published maps and institutional affiliations.